Chapter 1

In Vivo Whole-Cell Recordings

Bojana Kokinovic, Stylianos Papaioannou, and Paolo Medini

Abstract

The introduction of whole-cell, patch clamp recordings in vivo has allowed measuring the synaptic (excitatory and inhibitory) inputs and the spike output from molecularly or anatomically identified neurons. Combining this technique with two-photon microscopy also allows to optically target such recordings to the different subtypes of inhibitory cells (e.g., soma- and dendrite targeting), as well as to measure dendritic integration of synaptic inputs in vivo. Here we summarize the potentialities and describe the critical steps to successfully apply such an informative technique to the study of the physiology and plasticity of brain microcircuits in the living, intact brain.

Key words In vivo whole cell, Patch clamp, Brain microcircuits, Two-photon microscopy, Synaptic physiology

1 Introduction

Patch clamp pipettes have initially been used to measure the tiny currents that flow through single channels in voltage clamp [1]. Thereafter, patch clamp recordings have been used to record intracellular currents and voltages with the patch pipette in physical continuity with the cell cytoplasm (whole-cell configuration) [2]. Whole-cell recording remains the technique of choice to study synaptic connectivity and dynamics among visually identified cells in slices, by causing the occurrence of a spike in the presynaptic neurons while recording the postsynaptic response (paired whole-cell recordings) [3]. The use of patch electrodes to perform in vivo recordings has been carefully described by a seminal work done at Bert Sakmann's Lab [4]. Compared to sharp microelectrode recordings, whole-cell recordings have mainly the advantage that the access resistance is significantly lower, mostly due to the larger diameter of the pipette tip and the significantly shorter taper: this in turn allows smaller temporal distortions of fast electrical events, smaller voltage drops during current injections, and easier dialysis of the cytoplasm. The latter is a characteristic that turned

Alon Korngreen (ed.), *Advanced Patch-Clamp Analysis for Neuroscientists*, Neuromethods, vol. 113,
DOI 10.1007/978-1-4939-3411-9_1, © Springer Science+Business Media New York 2016

out to be useful for proper filling of cells with dyes (with the aim of neuroanatomical reconstructions) or with functional indicators (allowing for example dendritic calcium imaging in vivo—[5]). Another advantage in comparison with the sharp intracellular electrodes is that whole-cell electrodes do not rupture the neuronal membrane and hence cause less initial leakage of ions through it.

Here we will review the main potentials and the current limitations of the in vivo whole-cell recording techniques. We will stress the advantages of combining electrophysiological recordings with two-photon microscopy and optogenetics in the exploration of the physiology of cortical microcircuits in the living brain, with a concluding note on possible future developments of this technique. Finally, we present two experimental protocols related to the current use of this technique in our Lab: one to perform whole-cell recordings followed by neuronal anatomy in a functionally defined cortical area and one to perform two-photon targeted loose-patch recordings.

2 Potentialities

2.1 Simultaneous Measurements of Synaptic Inputs and Spike Outputs

In vivo whole-cell recordings allow simultaneous measurements of the synaptic inputs received by a neuron and of its spike output, during both spontaneous and sensory-driven activity. Indeed, the functional response properties of neurons are often different at sub- and suprathreshold level (Fig. 1). In general, response selectivity for stimulus features are sharper at action potential level: for example, in the primary visual cortex this is the case for orientation selectivity [6], binocularity [7], and segregation of ON and OFF subfields [8]. Also, comparison of synaptic and spike visual responses indicated that the reliability of the sensory responses is generally higher at the level of synaptic inputs [9, 10].

Blind in vivo whole-cell recordings are usually somatic [4]. However, recent work [11] demonstrated that it is possible to measure synaptic inputs with a patch pipette directly at the level of dendrites in vivo: importantly such work indicated that local, dendritic spikes contribute to the subthreshold orientation selectivity of V1 neurons.

2.2 Anatomical Reconstructions

By filling cells with biocytin it is possible to reveal the morphology and hence the anatomical identity of recorded cells by means of standard histochemical, peroxidase-based methods—e.g., [12]—see also Fig. 1. Slices can also be counterstained with cytochrome oxidase or with Nissl or myelin staining to reveal layering or other cytoarchitectonic features respectively. Both the dendrites and the axonal arbors of biocytin-filled cells can be reconstructed in 3D using a computer-assisted tracing system under 40× or

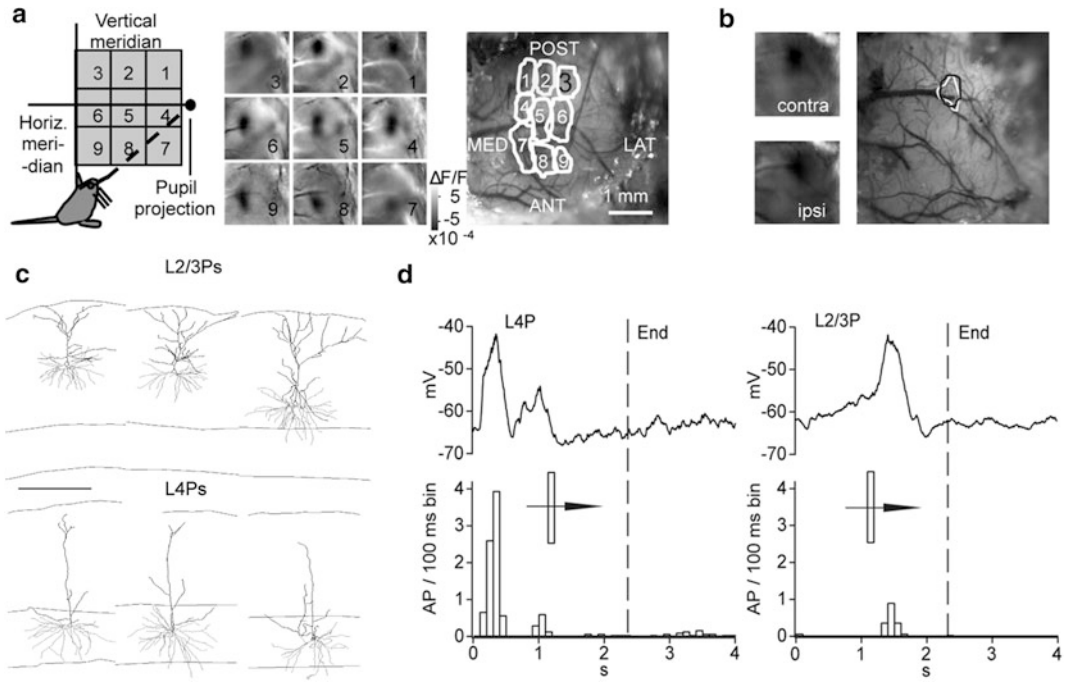

Fig. 1 Intrinsic optical imaging (IOI)-targeted in vivo whole-cell recordings of anatomically reconstructed layer 4 and layer 2/3 pyramids (L4Ps and L2/3Ps, respectively) in rat binocular V1. (**a**) Twenty-degree square spots displaying drifting gratings were randomly presented in different visual field positions (*left*). The corresponding IOI spots, representing the visually evoked focal decrease of light reflectance, were averaged over 40 stimulus presentations (*middle*), and overlaid on the vasculature image acquired before imaging with a green filter (*right*). All craniotomies were made over the IOI spot centered at 20° of elevation and neighboring the vertical meridian in the contralateral visual field (position 3, *red*), which corresponds to the center of the binocular region in the rat. (**b**) The two eyes were independently stimulated to confirm that the region of interest was located within the binocular portion of V1. Note the correspondence of the spots obtained through contralateral and ipsilateral eye stimulations in position 3. (**c**) Examples of coronal projections of the 3D reconstructions of basal (*red*) and apical (*black*) dendritic arbors of recorded L2/3Ps and L4Ps. Pial and layer 4 borders are outlined. Bar: 300 μm. (**d**) *L2/3Ps had similar PSP but smaller AP responses.* Examples of averaged PSP (*top* traces) and AP (*bottom* histograms) visual responses of a L4P (*left*) and of a L2/3P (*right*) to an optimally oriented moving light bar presented to the dominant eye. The bar starts sweeping the screen at time 0. *Dashed lines* indicate the beginning of the interstimulus period. From [10]

100× objectives. Such reconstructions can include also dendritic spines and axonal boutons quantification.

2.3 Estimate of Inhibitory and Excitatory Conductances

It is possible to estimate the excitatory and inhibitory components of synaptic responses by using in vivo whole-cell recordings [13–15]. This cannot be easily done by recording synaptic currents at the calculated reversal potentials for excitatory and inhibitory currents because of the space clamp problems—that prevent a homogeneous voltage clamping of all neuronal branches, and because depolarizing the cell at the reversal potential for excitatory currents can lead to uncontrolled activation of voltage-gated

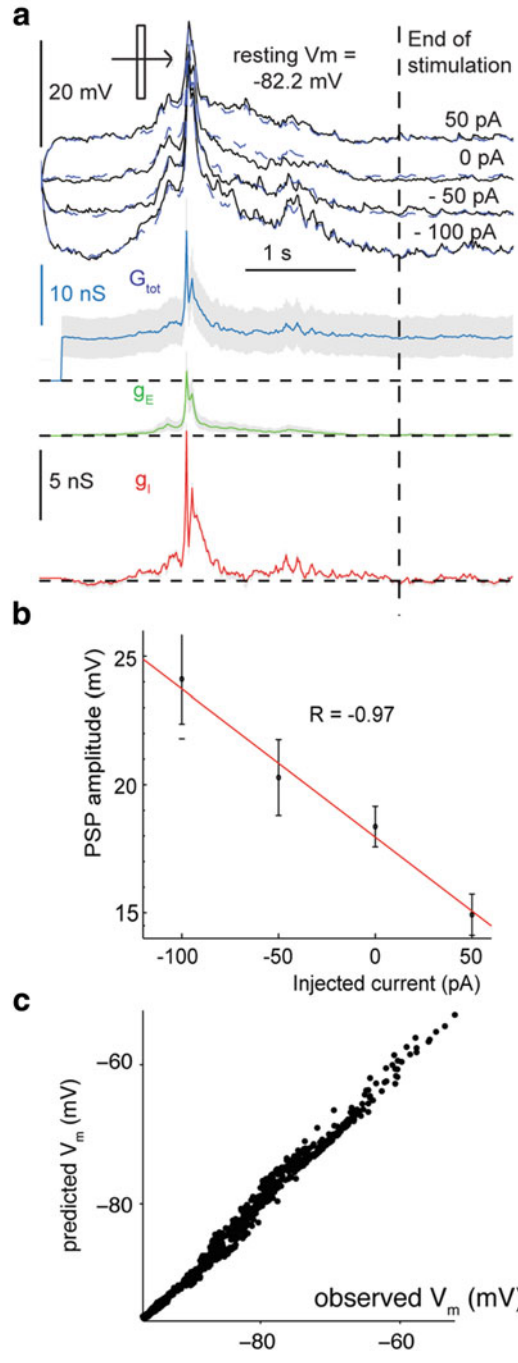

Fig. 2 Estimate of visually driven excitatory and inhibitory synaptic conductances. (**a**) Visual responses to an optimally oriented moving light bar of a layer 4 regular spiking neuron (4RSN) recorded under 1 mM QX314 while injecting different steady DC currents. The *black*, *continuous lines* are the recorded V_m values, whereas the *blue*, *dashed trace* shows the reconstructed V_m values obtained by inserting back the estimated g_E and g_I values into the fundamental membrane equation. The instantaneous total synaptic conductance

channels. For these reasons, excitatory and inhibitory conductances are usually estimated using a linear model of the membrane that assumes that the synaptic excitatory and inhibitory, as well as the nonsynaptic resting conductances, are largely voltage independent. This assumption must be carefully controlled, as there are clearly extrasynaptic, voltage-dependent conductances (e.g., I_h currents though HCN channels) as well as voltage-dependent synaptic conductances (e.g., NMDA channels). In the case of current clamp, the voltage response to sensory stimulation is recorded upon intracellular injection of different, mostly hyperpolarizing, current levels, a strategy to minimize the contributions of NMDA-receptor currents [16] as well as the activation of voltage-dependent channels (Fig. 2). A crucial point is controlling for the linearity of the current to voltage relation at the various injection steps, a prerequisite to apply this method. Preliminary to this calculation, the distortion of the voltage reading due to the series resistance must be corrected offline (Series resistance compensation) [17, 18]. The fundamental membrane equation is solved to extract the excitatory and inhibitory synaptic conductances as described in [19]. A further control for the linearity assumption is to reinsert back the values of excitatory and inhibitory conductances obtained in every point in time to see whether this predicts the actual membrane voltage values (membrane potential reconstruction). There are no significant differences in doing conductance estimates in current and voltage clamp, both in vitro and in vivo [16]. Also, blocking sodium and potassium voltage-active channels with intracellular QX-314 and Cs^+ helps in rendering neurons electrotonically more compact; however works in current clamp do not show significant differences

Fig. 2 (continued) is calculated based on the instantaneous slope of the current–voltage relation (G_{tot}, *blue*). The time-dependent excitatory (g_E, *green*) and inhibitory (g_I, *red*) conductances are plotted below. Gray traces represent the 95 % confidence intervals obtained by bootstrapping of the data. Conductance measurements began after the response to the injected current was at steady state (after 200 ms). Resting conductances were calculated in absence of visual stimulation (*dashed line*: stimulus end). (**b**) Visually driven PSPs vary linearly with the injected current. Plot showing the linearity of the relationship between the amplitude of the visually driven PSP response and the value of the injected current ($r = -0.97$) for a 4RSN (this plot refers to the example shown in Fig. 2 of the Main Text). Means $\pm$ standard errors are shown. The median of the correlation coefficients for all the recorded neurons was -0.94 (25th–75th percentiles: -0.88 to -0.99). (**c**) Plot of the recorded vs. reconstructed V_m values obtained by inserting back the estimated g_E and g_I into the membrane equation. The linearity of the cell and the accuracy of the V_m reconstruction are shown by the fact that data points align along the line of steepness 1 and intercept 0 in the plot. From [17]

between the conductance estimates when these blockers are added or omitted [17, 19].

When accurately controlled, the estimates of the excitatory and inhibitory conductances allow exploring the *temporal dynamics* of the excitatory and inhibitory synaptic inputs, and to put this in relation to the neuronal response. For example, work in the auditory cortex showed that after tone presentation excitation rises first and inhibition rises later, and that neuronal spiking occurs between the excitatory and inhibitory peaks, suggesting that the later inhibitory peak temporally confines the spiking, reducing its jitter [20]. Second, such methodology also allows the evaluation of the changes of the *relative strength* of the excitatory and inhibitory conductances, occurring for example, when a neuron is presented with the preferred or non-preferred orientation [13, 15], or after a change in the sensory environment, like monocular deprivation in area V1 [17, 21]. Indeed, the absolute conductance values obtained for inhibition and excitation can be affected by the different spatial distribution of the two types of synapses. For example, dendritic excitatory inputs are electrotonically more distant compared to perisomatic inhibitory contacts, a fact that is relevant because in vivo whole-cell recordings are mostly obtained from the soma.

2.4 Two-Photon Targeted Patch

Blind in vivo whole-cell patch recordings have a lower yield of inhibitory, non-pyramidal cells as compared to blind juxtasomal recordings and also in relation to the actual proportion of non-pyramidal, inhibitory cells (about 20 % of cortical neurons) (expected yield) [22, 23]. Two-photon targeted patch clamp has been introduced also for this purpose. The initial work indeed targeted GFP-labeled, parvalbumin-positive fast spiking cells in the cortex of transgenic mice using a patch pipette filled with a red fluorescent indicator [24]. This technique has been extensively used by the group of Carl Petersen to study the role of specific subpopulations of cortical interneurons in sensory processing in the primary somatosensory cortex—e.g., [25]. For example, such an approach showed that somatostatin-positive, dendritic targeting cells respond to whisker deflection in the barrel cortex with hyperpolarizations, a phenomenon that is not observed in any other cell type [26]. Several other Labs have used two-photon-targeted patching to perform loose-patch (juxtasomal) recordings from specific types of inhibitory neurons in both primary and association cortices. For example, this technique confirmed that the majority of parvalbumin-positive cells have scarcer orientation tuning in V1 compared to all remaining cortical neurons [27–29]. Also, in the multisensory (visuo-tactile) association cortex RL (Fig. 3), this technique showed a scarce multisensory integration in parvalbumin-positive cells, as compared to neighboring excitatory pyramidal neurons [30].

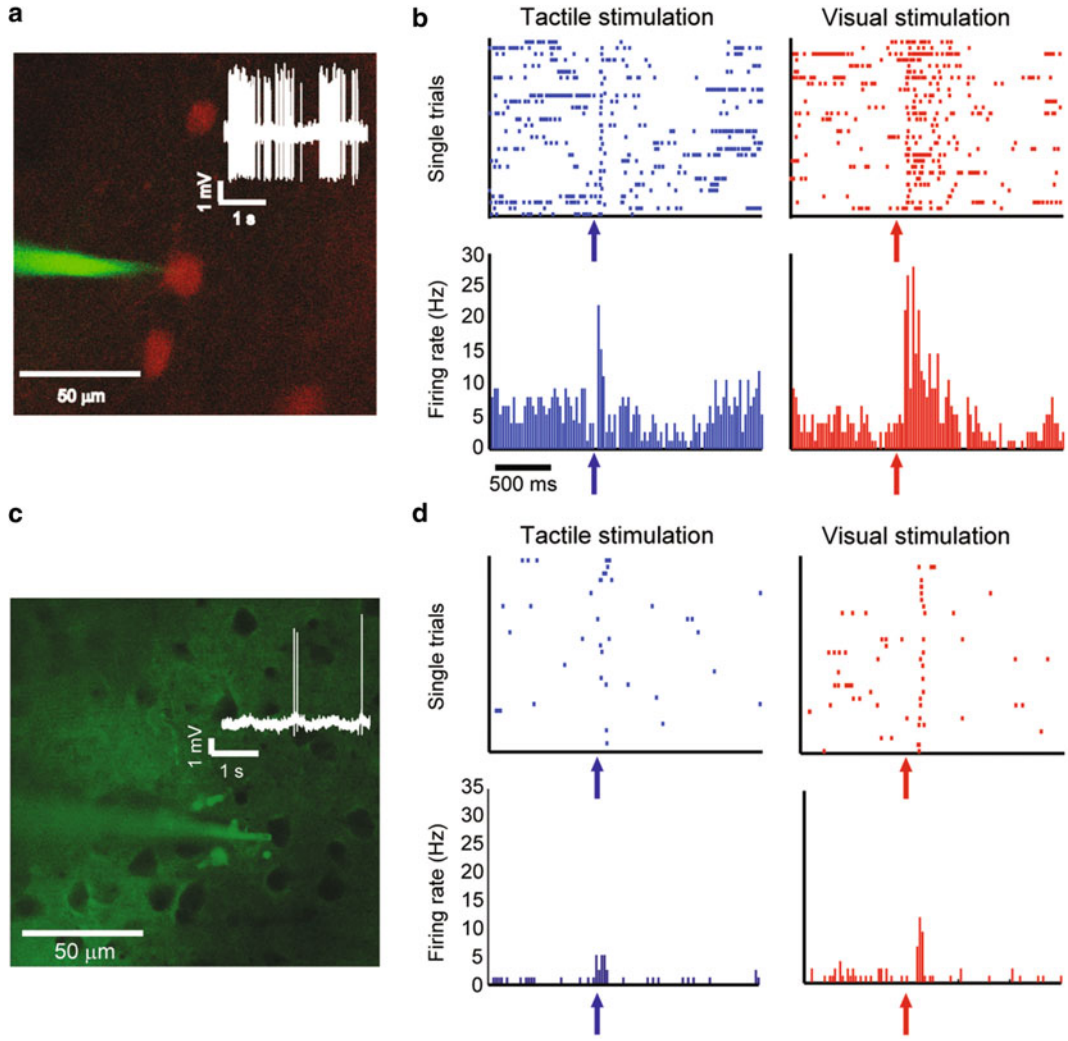

Fig. 3 Two-photon-targeted loose-patch recordings from inhibitory and excitatory neurons in the multisensory, visuo-tactile, mouse area RL. (**a**, **b**) Example raster plots (*top*) and peristimulus time histograms (*bottom*) for a two-photon-targeted juxtasomal recording of a bimodal Pv-IN upon tactile and visual stimulation (*blue* and *red*, respectively) from a mouse expressing the red protein tdTomato selectively in PV-INs (the pipette is filled with the green Na^{+}-salt dye Alexa488). Note the high frequency bursts of APs with pronounced after hyperpolarizations typical of PV-INs (*white*) *Arrows* are stimulus onsets. (**c**, **d**) Same as in (**a**, **b**) but for a regular-spiking pyramid targeted under the two-photon with the "shadow patching" technique (Alexa 488 being gently ejected in the extracellular matrix to visualize pyramidal cell bodies as *dark* structures). From [30]

2.5 Combining In Vivo Whole-Cell Recordings with Optogenetics: The Optopatcher

A second, interesting approach to record from specific cell types is the use of the so-called "optogenetic tags" realized with a conditional expression technique. Channelrhodopsin can be expressed in specific cell types by crossing mice that express the Cre recombinase in the aforementioned cell types with mice that bear a floxed-channelrhodopsin construct [31] (the latter construct can be also transduced into neurons by means of viral particles). In this case,

illumination of the cortical surface with an optic fiber stimulates specific cell types and this is used as a guide to evaluate whether the neuron facing the pipette tip belongs or not to the group of cells of interest. Such an approach has been recently used to compare the frequency tuning of parvalbumin-positive interneurons and of the excitatory pyramidal cells in the primary auditory cortex [32]. Also, this methodology is very promising to record from identified cell types in deep cortical layers or in deep subcortical structures that are not (yet) accessible to multiphoton microscopy. A recent development in this direction is provided by a modified version of the pipette holder that allows to guide the light coming from an optic fiber to the glass wall of the pipette until the very tip so to selectively illuminate the cell under recording (the so-called "optopatcher"—[33]).

2.6 Dendritic Physiology In Vivo

Patching a layer 2/3 cortical neuron with a pipette filled with the green fluorescent calcium indicator Oregon green BAPTA-1 allows to monitor calcium transients along the dendritic arbor [5] and even in single spines [34] in vivo. This technique requires a significant amount of time (more than 30 min) to allow proper dendritic filling of the previously patched neuron with the dye and benefits from using high-speed laser scanning system such as a resonant scanner [5], but can also be done with standard galvanometric mirrors on single dendritic stretches (Fig. 4). Patching the neuron is important because it allows the monitoring of the subthreshold (synaptic) response of the neuron (that are not captured by the calcium imaging) on one side, and also allows hyperpolarizing the cell to prevent the occurrence of somatic spikes. This is in turn important because a backpropagating spike in the dendrites can cause local calcium signals that can contaminate sensory-driven calcium transients.

Also, shadow patching under two-photon microscope guidance can aid to target patch clamp recordings to dendritic branches of cortical neurons: by using this approach Smith et al. showed the existence of sensory-driven dendritic spikes (independently of the occurrence of backpropagating action potentials) in vivo, and that such events influence the subthreshold tuning of visual cortical neurons as assessed by somatic recording [11].

2.7 Single-Cell, Intracellular Pharmacological and Genetic Manipulation

The relatively fast and efficient cytoplasmic dialysis of recorded neurons occurring during whole-cell recordings greatly facilitates intracellular perfusion with specific pharmacological agents or even with DNA plasmids for molecular manipulations. One example of the first case (pharmacological modulation) is given by experiments where intracellular NMDA blockers have been used to block dendritic spikes and to prove the role of these dendritic events in setting the angular tuning of layer 4 neurons in the barrel cortex [35], or by the intracellular perfusion of neurons with QX314 and Cs^+ to do conductance measurements—e.g., [19]. Another interesting application of genetic transduction of neurons with DNA plasmids

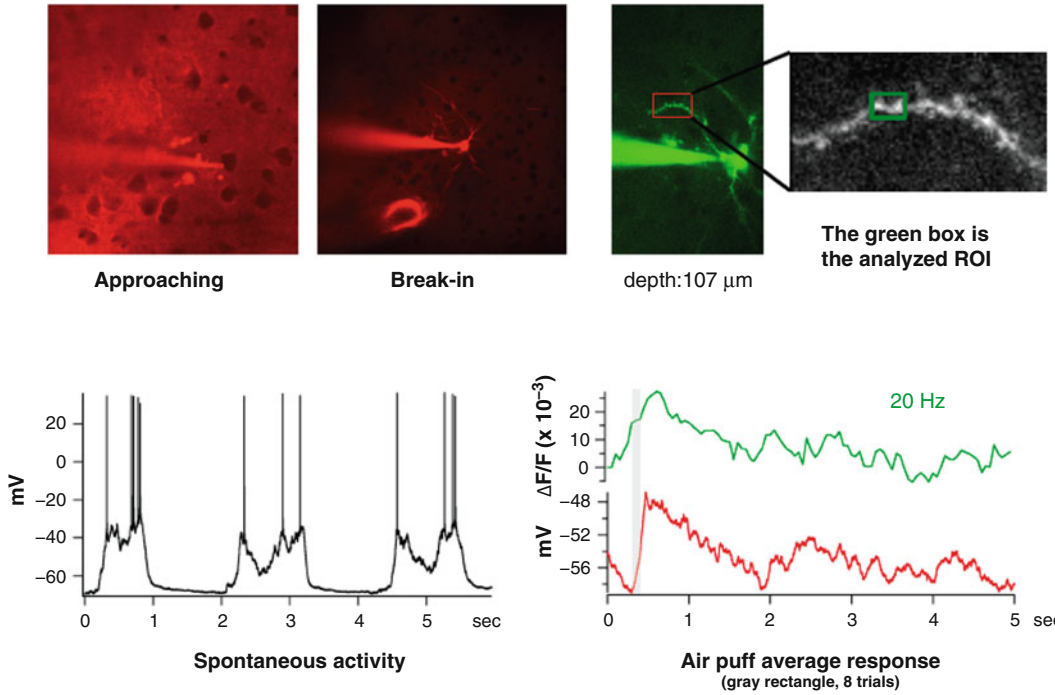

Fig. 4 Patching in vivo followed by dendritic calcium imaging in mouse barrel–somatosensory cortex to identify dendritic "hot spots." Top images: neurons are approached by using the shadow patching technique with the red Alexa 594 dye. The patch pipette is also filled with the green calcium indicator OGB-1, K+ salt, and the calcium imaging is done on the region of interest (ROI) on dendrites. *Bottom*: the *black* trace on the *left* represents the somatic voltage as recorded in current clamp. On the *right* plot the dendritic hot spot fluorescence response from the ROI (*green*) and the somatic voltage response (*red*) to whisker pad stimulation (Iurilli G and Medini P, unpublished data)

to study their microcircuits was given by a work of Rancz et al. [36]. In that work the authors used a set of plasmids in the recording pipette that restricted the retrograde transsynaptic labeling of afferent neurons only to the neurons that were monosynaptically connected with the recorded, transfected cell. Yet another application of single-cell labeling by means of plasmid transfection via the intracellular solution of the recording pipette is the ability to make time-lapsed in vivo whole-cell recordings from the same-tagged neuron. This technique brings the advantages of chronic recordings (follow the temporal evolution of response properties) into the armament of the intracellular electrophysiologist [37].

3 Current Limitations and Future Developments

The main current limitation of in vivo whole-cell recordings is represented by the limited sampling capability of the technique as compared to extracellular recordings or to two-photon population

calcium imaging. However, two considerations are relevant in this regard: (1) the variability of the functional response properties at subthreshold level is significantly lower than at suprathreshold (spike) level [9, 10]. So, synaptic responses are usually rather homogeneous within a given neuronal population (e.g., sound-driven hyperpolarization in layer 2/3 pyramidal neurons in V1 [18]; or tactile-driven hyperpolarizations in somatostatin-positive inhibitory interneurons in the somatosensory barrel cortex [26]). The fact that the synaptic responses are relatively homogeneous among a given population of cells in a given cortical layer is also proven by the fact that the synaptic responses of a single neuron are reflected with high fidelity by the local population voltage-sensitive dye response [38]. (2) In vivo whole-cell recordings can also be combined with extracellular recordings, with voltage-sensitive dye imaging or with two-photon imaging to measure also the population integrated synaptic response (e.g., VSD signal) and the population spike output (e.g., 2-photon calcium imaging). One representative example of how powerful and informative such a combined approach can be is given by experiments done by Randy Bruno and colleagues where a combination of extracellular recordings in the thalamus and in vivo whole-cell recordings in the cortex allowed measuring for the first time the unitary postsynaptic efficacy of thalamocortical synapses [39] and the synaptic strength of thalamic innervation in the different cell types composing columnar, excitatory microcircuits [40].

A second limitation is that in vivo whole-cell recordings are rather time-consuming and have a yield of a few neurons per animal on average. Of relevance, an automated system to perform non-human-assisted in vivo whole-cell recordings has been recently described. Such a system could allow a single human operator to simultaneously perform different sets of experiments on different animals (and rigs) [41].

A third limitation is that in vivo whole-cell recordings are currently done in immobile, anesthetized or awake, head-fixed rodents, cats, and recently even primates [42]. Importantly, the feasibility of in vivo whole-cell recordings in freely moving rodents has been at least demonstrated [43]. Further evolution will be needed to record neuronal activity intracellularly and chronically in freely moving animals. A very interesting evolution with respect to this might be represented by gold mushroom shaped microelectrode array that can be internalized—at least partially—by neurons to obtain intracellular-like recordings in vitro [44]. Developing proper technical approaches to implement a similar approach in vivo might allow important advances in this direction in the future.

4 Protocol for Intrinsic Signal Imaging-Targeted In Vivo Whole-Cell Recordings Followed by Anatomical Neuronal Identification

4.1 Animal and Surgical Preparation

Anesthetize the mouse with 20 % urethane (0.8–1 g/kg) i.p. (intraperitoneal). It is a long-lasting anesthetic that provides stable anesthesia conditions allowing keeping animals in spontaneous breathing. However, since it is carcinogenic, it is only allowed to be used for terminal procedures and must be handled accordingly.

Important: provide additional supplements of 10 % of the initial dose until the anesthesia depth foreseen in your Ethical Permit is reached. Anesthesia level should be repeatedly checked at the beginning of the experiment, and then regularly throughout the experiment, by observing the appearance of automatic movements (whisking, chewing) and by checking pinch and corneal reflexes. Absolutely avoid alarming signs that the level of anesthesia is insufficient such as piloerection and extensive salivation. In the recording setup, heart and breathing rate together with O_2 saturation should be carefully checked.

1. Place the mouse onto a heating plate (37 °C). It has to be kept in mind that anesthesia also impairs thermoregulation so it is crucial to carefully monitor and keep the body temperature (37 °C) of the animal during the whole procedure.
2. Inject dexamethasone intramuscularly (0.01 mg/kg). This prevents formation of brain and mucosal edemas.
3. Provide animal with a continuous supply of humidified oxygen through a nasal cannula.
4. Before surgery, infiltrate the skin with local lidocaine solution (1 %). With fine scissors, cut and remove the skin. With a fine spatula or a delicate bone scrapper also remove periosteum.
5. Place the recording chamber onto the exposed skull and fix it with the help of acrylic glue and dental cement. Pay attention to fix it on the skull firmly.
6. Gently thin the skull by using a drill until the blood vessels are clearly visible under the microscope. Stop drilling when you perceive that the bone has a "papyraceous" (i.e., paper-like) consistence and avoid drilling continuously in order to prevent friction-generated heat.

Intrinsic signal imaging can be done in case the in vivo whole-cell recordings need to be done in a precise position in the cortex. This procedure is more advisable than opening a large craniotomy and doing extracellular mapping because, for getting a good mechanical stability of the preparation, it is essential to open relatively small craniotomies (from 0.5 to 1 mm).

4.2 Intrinsic Signal Imaging Procedure and Craniotomy

1. Transfer the animal to the recording setup on a heating plate.
2. Acquire a vasculature ("green") image under 540 nm light. The diaphragms of the macroscope lenses should be kept closed in order to increase the depth of focus, minimize optical aberrations, and get the best possible image quality. Start imaging session by illuminating the cortex with monochromatic 630 nm light provided by stable DC current source. All images are acquired with a cooled CCD camera defocused ca 500–600 μm below the pial surface. Light intensity should be adjusted just below pixel saturation. To achieve this, completely open the bottom macroscope lens diaphragm.
3. Monitor the signal on line: for this purpose as well as for offline data analysis, divide the averaged images after stimulus presentation (allowing ca 1 s latency for the intrinsic signal to peak) by the average image before stimulus onset (Resting State Normalization). To analyze the spot extension, the ratio of the two images should be coded on a grayscale. In setting the clipping values, please remember that the intrinsic signal amplitude is usually about 1/1000 of the absolute reflected light. The region of interest ("spot area") can be reasonably taken as the image area where the stimulus-evoked decrease in reflectance is higher than 50 % of the peak decrease. This region has to be then overlaid with the vasculature "green" image by which location of craniotomy is determined.
4. The craniotomy should be cut with sharp blades (#11). In doing this there should be no bleeding and also no bone left. In general, stop any minimal bleeding coming from the nearby bone or dura mater by gently pushing some clotting cellulose sponge (e.g., Sugi®, Kettenbach, Germany) close to the bleeding point (but not *on* the damaged vessel).
5. Keep the craniotomy always moist by filling the recording chamber with warmed Ringer solution. In mice it is not necessary to remove the dura matter, whereas in rats it is: for this purpose, use a 33 gauge needle.

Advice: Pull your patch pipettes before opening the craniotomy (e.g., during the intrinsic imaging). Check the size and shape of the very tip of all your pipettes using a 100× air objective with a convenient working distance: the shape of the tip should be convex in order to maximize surface adhesion with cell membrane and the very final opening should be around 1 μm of diameter. Keep the pipettes protected from dust and use them no longer than the end of the day (cracks can appear on the pipette).

4.3 Patching In Vivo

1. Fill the patch pipettes with intracellular solution (in mM: 135 K gluconate, 10 HEPES, 10 Na phosphocreatine, 4 KCl, 4 ATP-Mg, 0.3 GTP, pH 7.2, 291 mOsm). In order to be

able to perform anatomical identification of the cell biocytin (3 mg/ml) can be added to the intracellular solution. The ideal resistance of the pipette for patching should be between 5 and 9 MΩ: this is the best compromise between having a reasonable probability to make a seal and having a reasonably low access resistance (<100 MΩ).

2. Apply positive pressure (300–400 mbar) using a 10-ml syringe in order to prevent occlusion of the pipette before touching the brain surface.
3. Dry the recording chamber from the Ringer solution and carefully approach the craniotomy surface until you touch the skull with the pipette tip.
4. Fill in the chamber again with Ringer solution.
5. Penetrate the dura—in case of mice—and the pia (only a temporary increase of the pipette resistance should be observed) and navigate through the cortex slowly while maintaining a high pressure level till the depth of interest is reached. Always keep the pipette resistance controlled while the amplifier is operating in voltage-clamp mode.
6. Once you have reached the depth of interest, decrease the pipette pressure to +30 mbar. In this way cells are not pushed away from the tip of the pipette.
7. Search for neurons in voltage clamp, monitor the current and pipette resistance, and while stepping the Z axis (step size = 2 μm), repeatedly null the pipette current to zero.
8. As the pipette gets closer to the cell, causing dimpling of its surface, the pipette resistance will increase (amplitude of the current pulse in voltage clamp decreases).

   Note that a slow increase in resistance probably does not indicate that the cells are being approached but rather means the tip is becoming clogged. When the resistance is approximately doubled and it is possible to see in the current trace heart-beat-associated pulsations (strokes) usually it is a sign that the pipette is leaning against a cell. Try to release the pressure while hyperpolarizing the pipette potential: in ideal conditions this leads to the spontaneous formation of a gigaseal. However, it is usually necessary to apply transient negative pressure (50–100 mbar) to promote gigaseal formation. Forming a gigaseal is usually a relatively fast process and if the seal is not formed within 1–2 min it is best to try with a new pipette. In case of failure slowly come out and try a new pipette.
9. After having established a seal compensate the fast capacitive artifacts. Avoid overcompensation that can lead to amplifier oscillation.

10. Membrane rupturing is done by a quick, negative pressure ramp: suddenly the slow exponential due to membrane capacitance charging will appear. At that point immediately release pressure. Switch to current clamp in "voltage follower" or "bridge mode."
11. It is highly advisable to also compensate the series resistant in order to minimize the voltage drop across the access resistance when current is injected (e.g., to estimate synaptic conductances). Series resistance compensation can also be done offline. Note: it is advisable, in case of pulsed sweep acquisition, to have a brief (e.g., 200 ms), slightly hyperpolarizing pulse (e.g., −100 pA) at the beginning or end of each sweep, first to allow for series resistance estimates as well as for monitoring it repeatedly during the experiment. *Tip:* Once a whole-cell configuration has been achieved, the duration of stable recordings can be increased by gently moving the pipette backward a few μm approx. every 30 min. In this way one can compensate for the initial displacement of the cell by the pipette during approach and gigaseal formation.

5 Troubleshooting

– If gigaohm seals cannot be obtained, there are a couple of probable causes that can be checked:

  First of all the health state of the animal: Are all vital signs within a physiological range (i.e., PCO2) (35 ± 3 mmHg) if the mouse is ventilated, heart rate (545 ± 78 beats/min) and body temperature (36.5–37.5 °C)? Next step is to check the shape and the size of the pipette tip. The resistance needs to be kept in the right range (5–9 MΩ). The pressure line to the pipette holder should be checked for leaks as well. Also osmolarity and pH of used intracellular solution should have proper value (see above).
– If gigaohm seals can be obtained but cannot be broken, or last for very short time, the pressure line to the pipette holder should be checked for leaks or obstructions. Moreover tuning the puller settings to improve pipette resistance and tip shape can be of great importance.
– Finding and eliminating sources of vibration is crucial to get gigaseals and for an acceptable duration of the recordings.

In general it is crucial to monitor animal health condition during experiment, all the vital signs need to be in physiological range, osmolarity of used solution must be appropriate, shape and size of used pipettes should be proper, and pressure line has to be without any leaks or obstruction.

5.1 Expected Results

If the animal is handled correctly and if the preparation was done in such a way to keep the vital signs under physiological condition, recordings can be obtained for more than 12 h. Moreover stable recordings from single neurons can be obtained for up to 3 h. Per day in general two to eight cells can be recorded.

5.2 Histological Procedure

1. Deeply anesthetize the mouse with urethane. Check if there is any responses to tail/toe pinches and also if there is any corneal reflex. Proceed only after the mouse is unresponsive and all of the above reflexes are absent.
2. Put the mouse inside a chemical fume hood in the supine position.
3. Perform transcardial perfusion with cold phosphate buffer saline (PBS 0.1 M, 20 ml) followed by aldehyde-based fixative (4 % paraformaldehyde in 0.1 M PBS, 60 ml).
4. Carefully extract the brain from the skull (first remove the dura mater).
5. Put the brain in aldehyde-based fixative overnight for postfixation.

5.3 Biocytin Staining Procedure

1. Cut 100–150 μm tick sections of brain using a vibratome.
2. Wash the slices three times in PBS, 10 min each.
3. Incubate the slices at 37 °C for 1 h in a solution of Cytochrome-c (300 μg/ml), Catalase (200 μg/ml), and Diaminobenzidine (0.5 mg/ml).
4. For stopping reaction wash the wells with bleach.
5. Wash the slices four times in PBS, 10 min each.
6. Quenching of endogenous peroxidase is done by incubating slices in a solution of 3 % hydrogen peroxide in PBS for 10–15 min.
7. Wash the slices five times in PBS, 10 min each.
8. Put the slices for one hour in a solution of Triton X-100 2 % in PBS for permeabilization of the slices.
9. Leave slices in solution of VECTASTAIN® ABC kit (sensitive avidin/biotin-based peroxidase system) (20 drops of A and 20 drops of B) and Triton X-100 1 % at 4 °C overnight, or for 2 h at room temperature.
10. Wash the slices five times in PBS, 10 min each.
11. For 15 min incubate slices in a solution of Diaminobenzidine (0.5 mg/ml) and 3 % hydrogen peroxide.
12. Wash the slices five times in PBS, 10 min each.

13. Mount the slices according to the order of sectioning on slides with mounting medium based on Mowiol-488, as it does not require dehydration.
14. Analyze the slices by using bright-field microscope. Screening for the slides containing the cell should be done with a 5× or 10× objective. Fine neuroanatomical analysis (and eventually neuronal reconstructions) should be done with a 40× or 100× objective. For the purpose of neuroanatomical reconstructions, it is highly advisable to patch only one or two (better one) neuron per craniotomy.

5.4 Two-Photon-Targeted Juxtasomal Recording

Two-photon targeted patching is a method which uses two-photon microscopy to optically target neurons that express fluorescent markers such as GFP variants or red fluorescent protein. Nevertheless, this method is restricted to mice expressing reporter proteins in identified cell types. However, it is possible to optically target patch recordings to genetically non-labeled neurons by using the shadow patching technique. The latter consists in ejection of a fluorescent dye in the extracellular space to visualize and approach the neuron cell bodies (with the possibility to distinguish pyramidal shaped and non-pyramidal shaped cells), because the dye is not taken up by the neuronal cells which appear like black (non-stained) objects on light (stained) background of the extracellular space, hence the name shadow patching.

With the same pipette that is used for delivering the fluorescent dye and guided by the two-photon microscope to individual shadowed cells, patch clamp can be performed. Since there is a constant flow of dye from the pipette, detecting when the pipette comes in contact with a neuron is possible due to a fluorescent cleft made in the cell membrane. If the suction is applied promptly the gigaseal or patch clamp in the cell membrane is formed. Here we will describe how we do two-photon targeted juxtasomal recordings in our lab [30].

5.5 Procedure

1. Perform the surgery of the animal as described. Be particularly careful not to cause any bleeding and not to produce too much heat during the drilling. Always administer systemic cortisone, provide oxygen, and carefully monitor the animal physiological parameters.
2. Fill the patch pipette with a solution of dye Alexa 594 (25 μm) in Ringer solution. The resistance of the pipette for shadow patching should be between 5 and 9 MΩ and should remain constant when lowering the pipette in the brain. Do not apply high pressure (300 mbar) on the pipette to avoid excessive spillover of the dye, particularly on the cortical surface. Use 20–40 mbar instead.

3. Tune the laser to a wavelength that is optimal for the dye used (e.g., 780–800 nm for Alexa 594).
4. Lower the pipette until layer 2/3 is reached (150–300 μm). Take into account the pipette angle in calculating the absolute depth. During the descent, move the pipette along its axis and move the objective focus to keep the pipette tip on the focal plane. To this purpose, it is useful to keep ejecting some dye in the surrounding tissue.
5. Apply small puffs of the dye (40–100 mbar). Provided that the pipette is not clogged, every pulse should label a volume of about 300 μm diameter. Cell somata should be instantaneously counterstained.
6. By moving the pipette in the $x - y$ plane with a micromanipulator slowly approach the cell of interest within 50 μm of pipette tip to avoid excessive tissue damage.
7. Approach the cell while monitoring seal resistance, the spike shape, and the microscope frame: juxtasomal configuration is reached when: (a) seal resistance is in the order of 30–100 MΩ; (b) the spike shape is positive and has a height of about 2 mV. Check if you can drive the cell to fire using a range of currents 1–5 nA [45]. During the experiment monitor the spike shape and the absolute value of voltage: spike broadening and a DC shift towards hyperpolarized values usually indicate cell damage. In that case one can observe labeling of the soma.

Two-photon microscopy can also be used to optically target non-labeled neurons by counterstaining the extracellular space with a fluorescent dye such as Alexa 594. In this way, neuronal cell bodies are visualized as black "holes" or shadows and the pipette can be advanced to the cell membrane so to patch the neuron ("shadow" patching—[46]). Significantly, three-dimensional reconstruction of the optical sections taken through a volume of tissue allows to target recordings to pyramidal shaped, excitatory cells or to non-pyramidal shaped, putative inhibitory neurons, thus allowing targeting different cell types even in the case of the unstained mammalian neocortex.

References

1. Neher E, Sakmann B (1976) Single-channel currents recorded from membrane of denervated frog muscle fibres. Nature 260(5554):799–802
2. Sakmann B (2006) Patch pipettes are more useful than initially thought: simultaneous pre- and postsynaptic recording from mammalian CNS synapses in vitro and in vivo. Pflugers Arch 453(3):249–259
3. Feldmeyer D, Sakmann B (2000) Synaptic efficacy and reliability of excitatory connections between the principal neurones of the input (layer 4) and output layer (layer 5) of the neocortex. J Physiol 525(Pt 1):31–39
4. Margrie TW, Brecht M, Sakmann B (2002) In vivo, low-resistance, whole-cell recordings from neurons in the anaesthetized and awake mammalian brain. Pflugers Arch 444(4):491–498. doi:10.1007/s00424-002-0831-z
5. Jia H, Rochefort NL, Chen X, Konnerth A (2010) Dendritic organization of sensory

input to cortical neurons in vivo. Nature 464 (7293):1307–1312
6. Carandini M, Ferster D (2000) Membrane potential and firing rate in cat primary visual cortex. J Neurosci 20(1):470–484
7. Medini P (2011) Layer- and cell-type-specific subthreshold and suprathreshold effects of long-term monocular deprivation in rat visual cortex. J Neurosci 31(47):17134–17148
8. Priebe NJ, Mechler F, Carandini M, Ferster D (2004) The contribution of spike threshold to the dichotomy of cortical simple and complex cells. Nat Neurosci 7(10):1113–1122
9. Carandini M (2004) Amplification of trial-to-trial response variability by neurons in visual cortex. PLoS Biol 2(9):E264
10. Medini P (2011) Cell-type-specific sub- and suprathreshold receptive fields of layer 4 and layer 2/3 pyramids in rat primary visual cortex. Neuroscience 190:112–126
11. Smith SL, Smith IT, Branco T, Hausser M (2013) Dendritic spikes enhance stimulus selectivity in cortical neurons in vivo. Nature 503(7474):115–120
12. Brecht M, Sakmann B (2002) Dynamic representation of whisker deflection by synaptic potentials in spiny stellate and pyramidal cells in the barrels and septa of layer 4 rat somatosensory cortex. J Physiol 543(Pt 1):49–70
13. Anderson JS, Carandini M, Ferster D (2000) Orientation tuning of input conductance, excitation, and inhibition in cat primary visual cortex. J Neurophysiol 84(2):909–926
14. Borg-Graham L, Monier C, Fregnac Y (1996) Voltage-clamp measurement of visually-evoked conductances with whole-cell patch recordings in primary visual cortex. J Physiol Paris 90 (3–4):185–188
15. Monier C, Chavane F, Baudot P, Graham LJ, Fregnac Y (2003) Orientation and direction selectivity of synaptic inputs in visual cortical neurons: a diversity of combinations produces spike tuning. Neuron 37(4):663–680
16. Monier C, Fournier J, Fregnac Y (2008) In vitro and in vivo measures of evoked excitatory and inhibitory conductance dynamics in sensory cortices. J Neurosci Methods 169(2):323–365
17. Iurilli G, Olcese U, Medini P (2013) Preserved excitatory-inhibitory balance of cortical synaptic inputs following deprived eye stimulation after a saturating period of monocular deprivation in rats. PLoS One 8(12):e82044
18. Iurilli G, Ghezzi D, Olcese U, Lassi G, Nazzaro C, Tonini R, Tucci V, Benfenati F, Medini P (2012) Sound-driven synaptic inhibition in primary visual cortex. Neuron 73 (4):814–828
19. Priebe NJ, Ferster D (2005) Direction selectivity of excitation and inhibition in simple cells of the cat primary visual cortex. Neuron 45 (1):133–145
20. Wehr M, Zador AM (2003) Balanced inhibition underlies tuning and sharpens spike timing in auditory cortex. Nature 426(6965):442–446
21. Ma WP, Li YT, Tao HW (2013) Downregulation of cortical inhibition mediates ocular dominance plasticity during the critical period. J Neurosci 33(27):11276–11280
22. Gonchar Y, Wang Q, Burkhalter A (2007) Multiple distinct subtypes of GABAergic neurons in mouse visual cortex identified by triple immunostaining. Front Neuroanat 1:3
23. Gonchar Y, Burkhalter A (1997) Three distinct families of GABAergic neurons in rat visual cortex. Cereb Cortex 7(4):347–358
24. Margrie TW, Meyer AH, Caputi A, Monyer H, Hasan MT, Schaefer AT, Denk W, Brecht M (2003) Targeted whole-cell recordings in the mammalian brain in vivo. Neuron 39 (6):911–918
25. Gentet LJ, Avermann M, Matyas F, Staiger JF, Petersen CC (2010) Membrane potential dynamics of GABAergic neurons in the barrel cortex of behaving mice. Neuron 65 (3):422–435
26. Gentet LJ, Kremer Y, Taniguchi H, Huang ZJ, Staiger JF, Petersen CC (2012) Unique functional properties of somatostatin-expressing GABAergic neurons in mouse barrel cortex. Nat Neurosci 15(4):607–612
27. Runyan CA, Schummers J, Van Wart A, Kuhlman SJ, Wilson NR, Huang ZJ, Sur M (2010) Response features of parvalbumin-expressing interneurons suggest precise roles for subtypes of inhibition in visual cortex. Neuron 67 (5):847–857
28. Kuhlman SJ, Tring E, Trachtenberg JT (2011) Fast-spiking interneurons have an initial orientation bias that is lost with vision. Nat Neurosci 14(9):1121–1123
29. Kerlin AM, Andermann ML, Berezovskii VK, Reid RC (2010) Broadly tuned response properties of diverse inhibitory neuron subtypes in mouse visual cortex. Neuron 67(5):858–871
30. Olcese U, Iurilli G, Medini P (2013) Cellular and synaptic architecture of multisensory integration in the mouse neocortex. Neuron 79 (3):579–593
31. Madisen L, Mao T, Koch H, Zhuo JM, Berenyi A, Fujisawa S, Hsu YW, Garcia AJ 3rd, Gu X, Zanella S, Kidney J, Gu H, Mao Y, Hooks BM, Boyden ES, Buzsaki G, Ramirez JM, Jones AR, Svoboda K, Han X, Turner EE, Zeng H (2012) A toolbox of Cre-dependent optogenetic

transgenic mice for light-induced activation and silencing. Nat Neurosci 15(5):793–802

32. Moore AK, Wehr M (2013) Parvalbumin-expressing inhibitory interneurons in auditory cortex are well-tuned for frequency. J Neurosci 33(34):13713–13723
33. Katz Y, Yizhar O, Staiger J, Lampl I (2013) Optopatcher – an electrode holder for simultaneous intracellular patch-clamp recording and optical manipulation. J Neurosci Methods 214 (1):113–117
34. Chen X, Leischner U, Rochefort NL, Nelken I, Konnerth A (2011) Functional mapping of single spines in cortical neurons in vivo. Nature 475(7357):501–505
35. Lavzin M, Rapoport S, Polsky A, Garion L, Schiller J (2012) Nonlinear dendritic processing determines angular tuning of barrel cortex neurons in vivo. Nature 490(7420):397–401
36. Rancz EA, Franks KM, Schwarz MK, Pichler B, Schaefer AT, Margrie TW (2011) Transfection via whole-cell recording in vivo: bridging single-cell physiology, genetics and connectomics. Nat Neurosci 14(4):527–532
37. Cohen L, Koffman N, Meiri H, Yarom Y, Lampl I, Mizrahi A (2013) Time-lapse electrical recordings of single neurons from the mouse neocortex. Proc Natl Acad Sci U S A 110(14):5665–5670
38. Petersen CC, Grinvald A, Sakmann B (2003) Spatiotemporal dynamics of sensory responses in layer 2/3 of rat barrel cortex measured in vivo by voltage-sensitive dye imaging combined with whole-cell voltage recordings and neuron reconstructions. J Neurosci 23 (4):1298–1309
39. Bruno RM, Sakmann B (2006) Cortex is driven by weak but synchronously active thalamocortical synapses. Science 312(5780):1622–1627
40. Constantinople CM, Bruno RM (2013) Deep cortical layers are activated directly by thalamus. Science 340(6140):1591–1594
41. Kodandaramaiah SB, Franzesi GT, Chow BY, Boyden ES, Forest CR (2012) Automated whole-cell patch-clamp electrophysiology of neurons in vivo. Nat Methods 9(6):585–587
42. Tan AY, Chen Y, Scholl B, Seidemann E, Priebe NJ (2014) Sensory stimulation shifts visual cortex from synchronous to asynchronous states. Nature 509(7499):226–229
43. Lee AK, Manns ID, Sakmann B, Brecht M (2006) Whole-cell recordings in freely moving rats. Neuron 51(4):399–407
44. Spira ME, Hai A (2013) Multi-electrode array technologies for neuroscience and cardiology. Nat Nanotechnol 8(2):83–94
45. Pinault D (1996) A novel single-cell staining procedure performed in vivo under electrophysiological control: morpho-functional features of juxtacellularly labeled thalamic cells and other central neurons with biocytin or neurobiotin. J Neurosci Methods 65(2): 113–136
46. Kitamura K, Judkewitz B, Kano M, Denk W, Hausser M (2008) Targeted patch-clamp recordings and single-cell electroporation of unlabeled neurons in vivo. Nat Methods 5(1):61–67